Liquid Crystals
Publication details, including instructions for authors and subscription information:
http://www.informaworld.com/smpp/title~content=t713926090

Induced crystal G phase through intermolecular hydrogen bonding VII. Influence of non-covalent interactions on mesomorphism and crystallization kinetics

M. Srinivasulu; P. V. V. Satyanarayana; P. A. Kumar; V. G. K. M. Pisipati

Online publication date: 06 August 2010

To cite this Article Srinivasulu, M. , Satyanarayana, P. V. V. , Kumar, P. A. and Pisipati, V. G. K. M.(2001) 'Induced crystal G phase through intermolecular hydrogen bonding VII. Influence of non-covalent interactions on mesomorphism and crystallization kinetics', Liquid Crystals, 28: 9, 1321 — 1329
To link to this Article: DOI: 10.1080/02678290110062231
URL: http://dx.doi.org/10.1080/02678290110062231

LIQUID CRYSTALS, 2001, VOL. 28, NO. 9, 1321–1329

Induced crystal G phase through intermolecular hydrogen bonding VII. Influence of non-covalent interactions on mesomorphism and crystallization kinetics†

M. SRINIVASULU, P. V. V. SATYANARAYANA

Department of Chemistry, Faculty of Physical Sciences, Nagarjuna University, Nagarjuna Nagar 522 510, India

P. A. KUMAR and V. G. K. M. PISIPATI*

Centre for Liquid Crystal Research and Education, Faculty of Physical Sciences, Nagarjuna University, Nagarjuna Nagar 522 510, India

(*Received 1 February 2001; accepted 13 March 2001*)

A series of intermolecular hydrogen bonding complexes, 2,2′-bipyridine : *p-n*-alkoxybenzoic acids (BP : *n*ABA) was isolated from liquid crystalline *p-n*-alkoxybenzoic acids (*n*ABA) (where *n* represents alkoxy carbon numbers, 3 to 10 and 12) and a non-mesogen, 2,2′-bipyridine (BP). The thermal and phase behaviour of these complexes was studied by thermal microscopy and differential scanning calorimetry (DSC). These studies revealed the induction of tilted smectic F and crystal G phases. The structural elucidation pertaining to the formation of intermolecular hydrogen bonding was carried out by a detailed IR spectral investigation. Comparative crystallization kinectic studies using DSC, performed on two representative compounds, showed different forms of the crystallization process. The magnitudes of the Avrami exponent *n* suggests two different mechanisms operate for individual members leading to sporadic three-dimensional growth. Nevertheless, an overall unique mechanism is predicted to operate at each crystallization temperature investigated, while the Avrami constant *b* shows a temperature dependence suggesting a strong influence of alkoxy terminal groups on the rates of nucleation.

1. Introduction

Recently much interest has been generated among material chemists on the formulation of novel liquid crystal systems containing intermolecular hydrogen bonds, due to their significant role in mesomorphic morphology [1–6]. Since the discovery of a H-bonded liquid crystal compound by Kato and Frechet [7], the realization of the striking influence of these non-covalent interactions on mesomorphic behaviour has led to a new era in the fascinating discipline of liquid crystals. Interest in these H-bonded materials also arises from their low bond and activation energies: this is considered to be the basis for the origin of new stable mesophases with wide thermal spans. These non-covalent interactions have a pronounced influence on the rate of crystallization and the related parameters involved in the process of nucleation [8–10].

*Author for correspondence;
e-mail: venkatapisipati@hotmail.com
†For part VI see ref. [9].

In general, a phase transition from one distinct phase to another may be considered as the transformation from one completely ordered phase to another ordered phase. During such a transition, however, the co-existence of phases in each other's matrix may be likened to a disordered phase. Thus, the process of transformation consists of the growth of one species at the expense of the other, passing through a state of what may be approximately likened to maximum disorder. The transformation from phase I to phase II can be considered as occurring by two routes: (*a*) the *nucleation step* involving a spontaneous conversion of some isolated units of phase I into phase II when it is not surrounded by II and (*b*) the *propagation step* ascribed to the conversion of phase I to phase II at I–II interfaces, where the activation energy for conversion is likely to be low. Nevertheless, both these nucleation and propagation steps are solely dependent on nucleation and growth rates. As phase II grows inside the matrix of phase I, the growth continues until such time as phase I impinges on a growth barrier such as domains or free surfaces.

Liquid Crystals ISSN 0267-8292 print/ISSN 1366-5855 online © 2001 Taylor & Francis Ltd
http://www.tandf.co.uk/journals
DOI: 10.1080/02678290110062231

In fact, in conventional liquid crystals, the process of crystallization takes place when a stable lower temperature phase grows out of a mother metastable phase in the form of small domains, which are manifested equally by temperature and time. This nucleation process, however, leads to the formation of an ordered domain, which in turn converts to a stable nucleus that triggers the aggregation of the surrounding molecules to form layered domains. However, the H-bonded systems under study exhibit an altogether different mode in the distribution of heat transformation, and hence it is quite reasonable to expect the formation of a growing domain across the molecular layers, solely dependent on the strength of hydrogen bonding with respect to temperature. In order to understand such a nucleation mechanism in these non-covalent systems, the study of crystallization kinetics serves as a powerful tool.

In continuation of our previous efforts on crystallization kinetics using DSC [8–10], the present communication deals with the thermal and phase behaviour of the intermolecular hydrogen bonding complexes, 2,2′-bipyridine: *p-n*-alkoxybenzoic acids (BP:*n*ABA) (figure 1), isolated from the non-mesogenic 2,2′-bipyridine (BP) and liquid crystalline *p-n*-alkoxybenzoic acids (*n*ABA) (where *n* represents alkoxy carbon numbers, 3 to 10 and 12). This paper also presents comprehensive results on the comparative crystallization kinetic experiments performed on two representative compounds, BP:7ABA and BP:8ABA.

2. Experimental

2.1. *Materials and methods*

All the substituted *p-n*-alkoxybenzoic acids (of 99.9% purity) were supplied by Frinton Laboratories, New Jersey, USA while the non-mesogen, 2,2′-bipyridine was procured from Sigma Chemical Company, USA. Pyridine was purified by a standard literature method [11]. The IR spectra in solid and dissolved states were recorded on a Perkin-Elmer FTIR spectrometer.

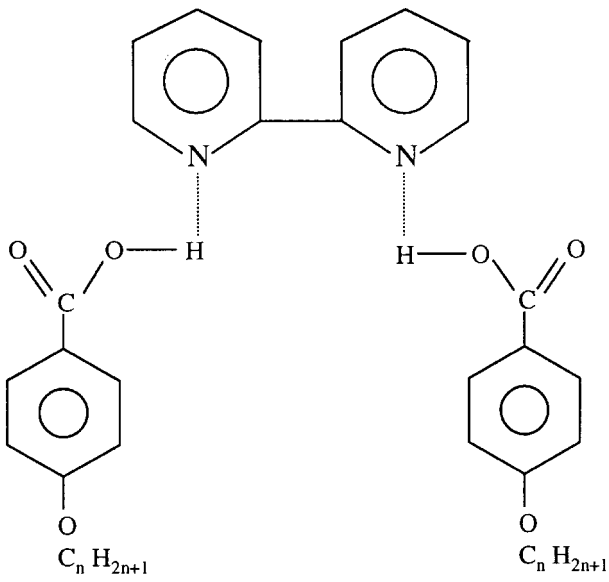

Figure 1. Molecular structure of 2,2′-bipyridine:*p-n*-alkoxybenzoic acid complexes.

The phase variants and their transition temperatures of free *p-n*-alkoxybenzoic acids and the corresponding series of intermolecular hydrogen-bonded complexes were determined from the characteristic textural observations by polarized microscopy (Hertel-Reuss [12] with super pan-II and Olympus BX-50 microscopes) at a scan rate of 0.1°C min^{-1}. The temperatures of the corresponding phase transitions and their heats of transitions (in J g^{-1}) were further measured from DSC thermograms (Perkin-Elmer DSC7) performed at a scan rate of 5°C min^{-1}. The phase behaviour of the H-bonded complexes is discussed in comparison with free *p-n*-alkoxybenzoic acids.

The crystallization kinetics relating to the transition from crystal phase to melt for each compound was selectively performed at each predetermined crystallization temperature. The method of thermal selectivity of crystallization temperatures and a typical DSC thermal scan at each crystallization temperature is described as reported earlier [8].

2.2. *Synthesis of 2,2′-bipyridine:p-n-alkoxybenzoic acids (BP:nABA)*

The intermolecular H-bonded complexes of BP:*n*ABA were synthesized by mixing together the appropriate *p-n*-alkoxybenzoic acid (40 mmol) and 2,2′-bipyridine (3.1 gm, 20 mmol) in absolute pyridine (~20 ml). The mixture was stirred under reflux for 6 h. The white/pink crystalline crude complexes were obtained by removing excess pyridine under vacuum distillation. The crude complexes were then recrystallized from hot dichloromethane and dried over calcium chloride in a desiccator at room temperature to give a yield of ~94%.

3. Results and discussion

All the complexes isolated under the present investigation are white/pink crystalline solids and are stable at room temperature. They are insoluble in water and sparingly soluble in common organic solvents such as methanol, ethanol, benzene and dichloromethane. However, they show a high degree of solubility in coordinating solvents such as dimethylsulfoxide (DMSO), dimethylformamide (DMF) and pyridine. All these complexes melt at specific temperatures below 155°C (table 1). They show high thermal and chemical stability when subjected to repeated thermal scans performed during thermal microscopy (TM) and DSC studies.

Table 1. Transition temperatures (°C) by TM; transition temperatures (°C) and enthalpies ($J\,g^{-1}$) by DSC in square brackets.

		Phase transition				
BP:*n*ABA (*n*)	Phase variant	I–N/G	N–C/G	C–F/G	F–G	G–Cr
I (3)	G	154.2 [153.8 (8.4)]				138.4 [137.6 (62.2)]
II (4)	N	140.1 [136.6 (85.5)]				133.5 [129.5 ([a])]
III (5)	N	147.0 [150.3 (5.44)]				110.2 [113.7 (64.1)]
IV (6)	N	150.0 [151.9 (8.49)]				93.8 [94.9 (50.4)]
V (7)	NCG	147.0 [146.6 (8.49)]	100.2 [97.2 (8.1)]	90.1 [88.0 (52.4)]		86.0 [83.2 (75.6)]
VI (8)	NCG	143.0 [139.6 (7.9)]	93.6 [89.0 (27.8)]	88.1 [86.8 ([a])]		56.0 [53.2 (54.1)]
VII (9)	NCG	122.2 [121.6 (10.7)]	95.0 [94.1 ([a])]	85.3 [84.7 (29.4)]		63.1 [62.7 (75.0)]
VIII (10)	NCFG	135.0 [135.0 ([a])]	116.2 [114.3 (1.4)]	97.5 [95.3 (1.8)]	87.7 [86.2 (27.2)]	75.1 [73.6 (22.2)]
IX (12)	NCFG	128.0 [128.1 (2.7)]	124.1 [123.3 (2.2)]	116.0 [113.0 ([a])]	84.8 [81.9 (21.8)]	65.9 [66.4 (4.5)]

[a] Transition peaks are not well resolved.

3.1. *IR spectra*

The IR spectra of *p*-*n*-alkoxybenzoic acids, *n*ABA, were recorded at room temperature in both the solid (KBr) and dissolved (chloroform) states. The spectra of free *p*-*n*-alkoxybenzoic acids show two sharp bands at 1685 and 1695 cm^{-1} due to the ν(C=O) mode and a band of strong intensity at 3032 cm^{-1} assigned to the ν(OH) mode of the carboxylate group. This doubling nature of the carbonyl stretching mode may be attributed to the existence of dimeric *n*ABA at room temperature [2, 6]. However, the corresponding spectra recorded in chloroform solution show a band of strong intensity at 1712 cm^{-1} suggesting the stabilization of the monomeric form of benzoic acid in solution. To avoid further complications due to such intermolecular interactions, comparisons of the spectra of complexes were made with the solution state spectra of free *n*ABA. The solid state (nujol mull) spectrum of free 2,2′-bipyridine (BP) shows two bands of medium intensity at 733 and 758 cm^{-1} due to pyridine ring deformation modes [13].

The infrared frequencies of BP:*n*ABA show the presence of a band of strong intensity due to the ν(C=O) mode of benzoic acid at ~1675 cm^{-1}. This supports evidence of an ABA moiety in a monomeric form upon complexation. The formation of intermolecular hydrogen bonding between the ring nitrogens of 2,2′-bipyridine and the −COOH group of ABA in 1:2 BP:*n*ABA complexes can be explained on the basis of bathochromic shifts (~30 cm^{-1}) in the ν(C=O) mode of acid, and hypsochromic shifts (~50 cm^{-1}) in the pyridine ring deformation modes. Moreover, the absence of a band associated with the ν(OH) mode of the carboxylic acid group in the present complexation strongly supports the existence of H-bonding. The presence of intermolecular H-bonding is further inferred from the appearance of a new band with medium intensity at ~2920 cm^{-1}, diagnostic of a ν(H----N) mode in all the present series [14].

3.2. *Thermal and phase behaviour*

Optical microscopy reveals that *p*-*n*-alkoxybenzoic acids exhibit the nematic (marble) as a unique mesophase in the lower homologues ($n = 3$ to 6) and smectic C (schlieren) in higher members of the series. The phase transition temperatures observed through TM are found to be in reasonable agreement with the corresponding DSC data. The general phase behaviour of *n*ABA compounds is depicted in figure 2 in the form of a phase diagram constructed for alkoxy carbon numbers vs. transition temperatures. The thermal range of the smectic C phase increases with simultaneous quenching of the nematic phase [2, 6] with the increase of alkoxy chain length.

The optical microscopy observations imply that the BP:*n*ABA series exhibits nematic (N), smectic C (SmC), smectic F (SmF) and crystal G (G) phases. On cooling, the formation of the N phase begins as small droplets, followed on further cooling by the formation of a threaded marble texture. The transition from N to SmC is recorded on the basis of the appearance of a homeotropic schlieren texture. On further cooling, the formation of a yellow broken focal-conic fan texture in complexes

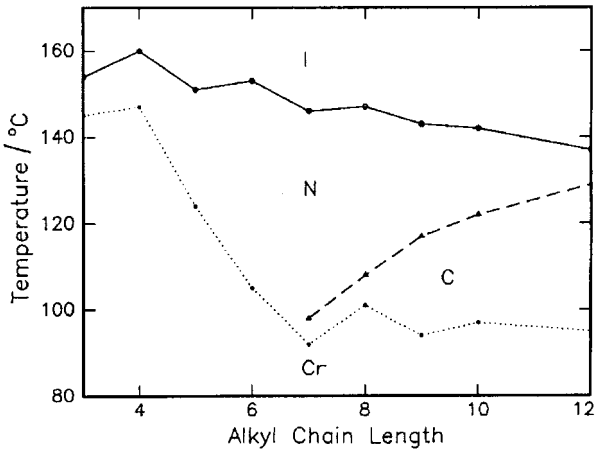

Figure 2. Phase diagram of *p-n*-alkoxybenzoic acids.

VIII and IX (with $n = 10$ and 12) confirms the phase transition from SmC to an induced SmF. In the complexes with $n = 3$ and 7 to 12, the induction of a G phase is assigned from the appearance of a smooth multicoloured mosaic texture. The phase transition temperatures observed by thermal microscopy are found to be in reasonable agreement with the corresponding DSC thermograms (table 1).

The thermal and phase behaviour of the BP:*n*ABA series is illustrated in the phase diagram shown in figure 3. This clearly suggests that the thermal span of the N phase is unaffected among middle members of the series. The existence of the induced G phase follows an interesting path that: in complex I it has a thermal span of ~15°C, followed by non-existence in the middle members, and then gradual reappearance in the higher homologues. In another sense, the thermal distribution

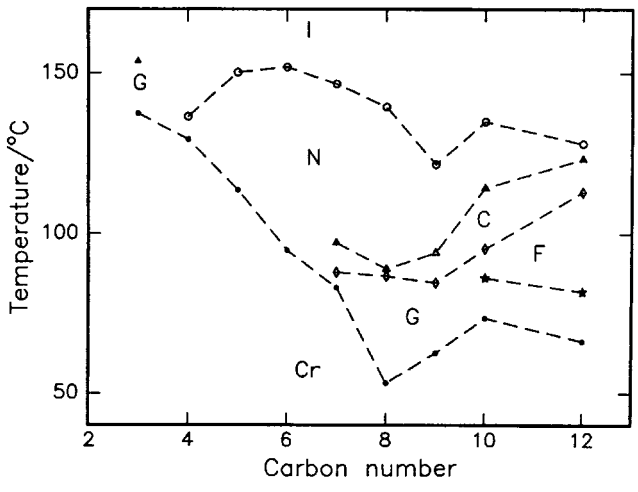

Figure 3. Phase diagram of 2,2′-bipyridine:*p-n*-alkoxybenzoic acid complexes.

of the N, which is a dominant phase in free *p-n*-alkoxybenzoic acids, is unaffected in the lower members of the series ($n = 4$ to 7). However, the thermal range of the G phase is balanced by another induced tilted phase (SmF) in complexes VIII and IX. As expected, the thermal range of liquid crystallinity is increased in the members of the present series in comparison with the free ABA series. Moreover, complex VI shows a wide thermal range of liquid crystallinity (~82°C).

The maximum thermal ranges of the induced phases G and SmF are observed for complexes VI (~33°C) and IX (15.5°C) respectively. The stabilization of these induced phases among the individual members of the series clearly suggests the effective role of hydrogen bonding associated with the electron-rich heteroatom (nitrogen) of the bipyridyl moiety and an ABA acid group. At this stage, it is reasonable to recall the thermal distribution of the induced G phase among the reported analogous complexes [9] derived from 2-amino-5-chloropyridine (non-mesogen moiety), where a gradual quenching of this phase is clearly observed in the higher homologues. Nevertheless, one cannot rule out steric contributions to the phase behaviour, associated with the bulky bipyridyl moiety. A noteworthy feature in the phase behaviour of higher homologues (figure 3) is the existence of the SmC phase and the decrease of the N thermal range. It is interesting to add that the compounds with carbon number 10 and 12 show all the mesophases, and that the present series exhibits an odd–even effect with respect to the thermal range of liquid crystallinity.

3.3. *Crystallization kinetics*

A systematic kinetic study of crystallization was performed on two individual members of the series, BP:7ABA and BP:8ABA. This study helps us to understand the influence of alkoxy chain length of the benzoic acid moiety on the rate of crystallization.

3.3.1. *BP:7ABA*

DSC thermograms of BP:7ABA scanned in heating and cooling cyles are summarized in figure 4. The heating scan shows three pertinent transitions at 95.1, 100.4 and 149.4°C with the corresponding enthalpies 135.9, 8.2 and 7.9 J g^{-1}, which are assigned, respectively, to Cr–melting, SmC–N and N–I phase transitions. On cooling the sample from its isotropic melt, the exotherm exhibits transitions due to I–N (146.6°C), N–SmC (97.2°C), SmC–G (88.0°C) and G–Cr (83.2°C) with the corresponding ethalpies 8.4, 8.1, 52.4 and 75.6 J g^{-1}, respectively. As suggested by the existing thermal range between the melting endotherm and crystal exotherm, the crystallization kinetics relating to the transition from the G phase was selectively performed at crystallization

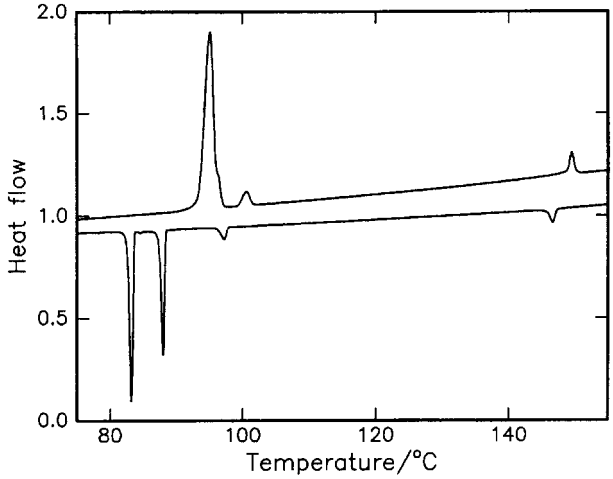

Figure 4. DSC endotherms and exotherm of 2,2′-bipyridine: *p-n*-heptyloxybenzoic acid complex.

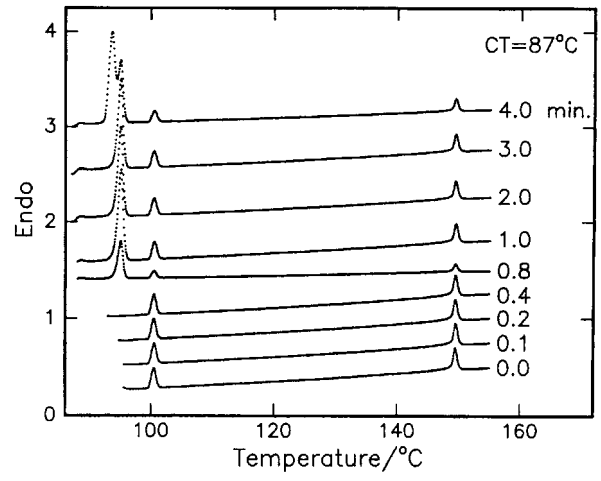

Figure 6. DSC endotherm profiles of 2,2′-bipyridine: *p-n*-heptyloxybenzoic acid complex at 87°C for different time intervals.

temperatures, 84, 85, 86 and 87°C. Typical endotherm profiles for different time intervals at crystallization temperatures 84 and 87°C are represented in figures 5 and 6, respectively.

The compound was held at 84°C for different time intervals (0.1 to 2.0 min). The heating curve was recorded at crystallization time of $t = 0$ min, following the quenching of the crystal-to-melting transition at crystallization temperature 84°C. This profile displays only G–N and N–I transitions, indicating the non-existence of a Cr–melting transition. However, after holding the sample for 0.1 min, a Cr–melting transition begins to appear, which clearly suggests a fast crystallization process. This melting peak increases with increasing time interval up to 2.0 min, where the enthalpy of the melting transition attains a saturated value. This process of crystallization can be explained on the basis of the formation of larger and larger crystal fractions with time, and this conversion process in the present case appears to be complete after 2.0 min. The endotherm profiles recorded at crystallization temperatures 85, 86 and 87°C for different time intervals showed a similar trend of crystallization kinetics and saturated enthalpy values were obtained after 2.0, 2.0 and 4.0 min, respectively. A noteworthy feature of the endotherm profiles at the final time intervals is the appearance of a shoulder in the melting peak. This may suggest the existence of two crystal fragments at the melting transition, with a competition between the two major fragments within the crystallization time scale (figures 5 and 6).

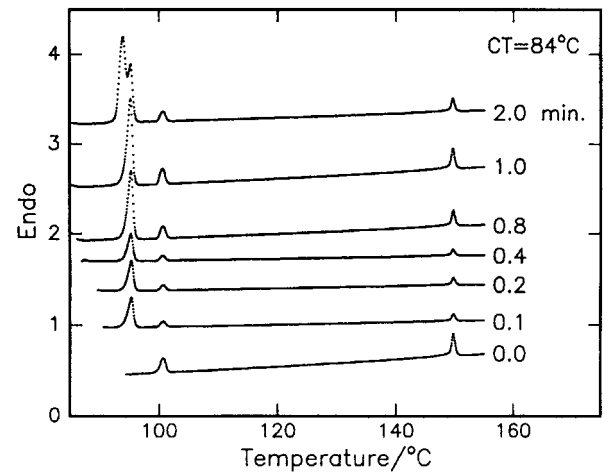

Figure 5. DSC endotherm profiles of 2,2′-bipyridine: *p-n*-heptyloxybenzoic acid complex at 84°C for different time intervals.

3.3.2. *BP:8ABA*

The DSC thermograms of BP:8ABA are illustrated in figure 7. On heating, the compound exhibits four distinct transitions at 57.5°C (Cr–Cr), 77.0 (Cr–melting), 96.1°C (G–SmC) and 140.1°C (N–I) with heats of transition 16.5, 60.4, 31.1 and 2.7 J g^{-1}, respectively. The cooling exotherm shows corresponding transitions at 138.1°C (I–N), 89.0°C (SmC–G), 53.1°C (G–Cr) with their enthalpy values 7.8, 27.8 and 54.1 J g^{-1}, respectively. The N–SmC transition could not be resolved either on heating or on cooling. These DSC thermograms indicate that the kinetics of crystallization from the G phase could be investigated between 51 and 55°C.

Figures 8 and 9 illustrate typical DSC endotherm profiles for different time intervals at crystallization temperatures, 51 and 55°C, respectively. As shown in figure 8, the sample was held at 51°C for different time intervals. The heating curves recorded after 0.1, 0.2, 0.4, 0.8, 1.0 and

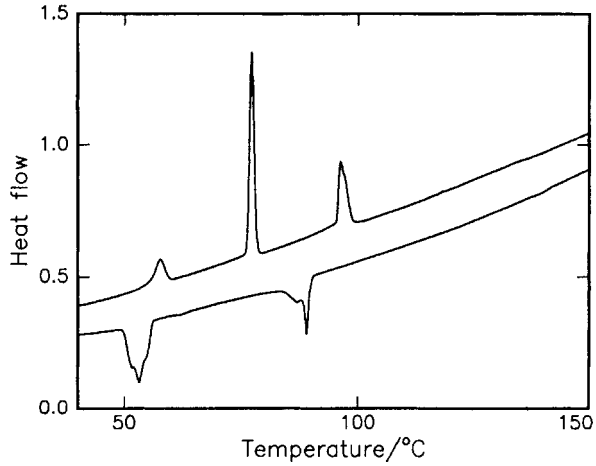

Figure 7. DSC endotherm and exotherm of 2,2′-bipyridine: *p-n*-octyloxybenzoic acid complex.

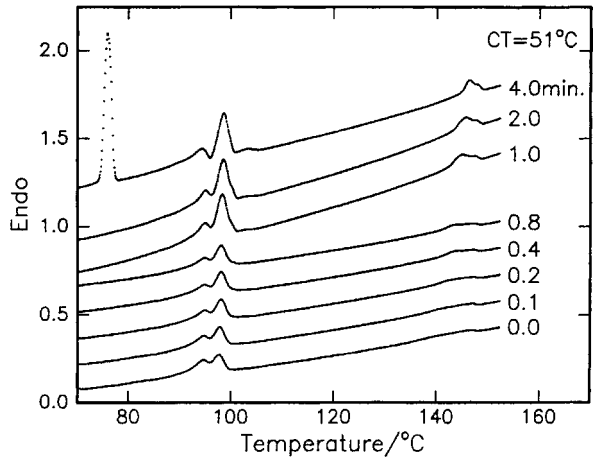

Figure 8. DSC endotherm profiles of 2,2′-bipyridine: *p-n*-octyloxybenzoic acid complex at 51°C for different time intervals.

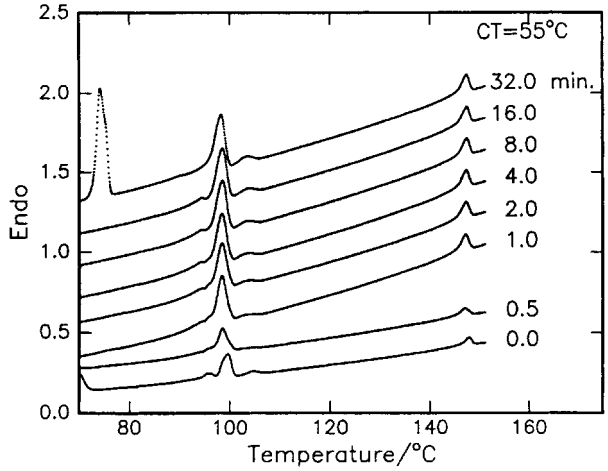

Figure 9. DSC endotherm profiles of 2,2′-bipyridine: *p-n*-heptyloxybenzoic acid complex at 55°C for different time intervals.

2.0 min show no Cr–melting transition. However, the sudden appearance of a melting transition is observed, with a saturated enthalpy value, after holding the sample for 4.0 min, which suggests a fast crystallization process as in the case of BP:7ABA. Experiments performed at different crystallization temperatures (52–55°C) show a similar trend of formation of the Cr–melting transition.

At this point, it is reasonable to predict that the compound BP:8ABA would exhibit a different trend in the formation of a melting transition with time having a negligible influence on its growth. However, the overall growth of crystallization is equally affected by both temperature and time. It is reasonable to recall the trend in the growth of the melting transition in BP:7ABA where it gradually increases with time. This provides substantial evidence towards the existence of an altogether different crystallization mechanism operating with the variation of alkoxy chain length of the benzoic acid moiety. Normally, in any relatively fast crystallization process the distribution of embryos (crystal domains) must re-establish a characteristic equilibrium in terms of both number and size which in turn leads to the phenomenon of 'incubation time', and no phase transformations could occur during such intervals. The occurrence of these incubation times is considered to be a common feature in many isothermal transformations [15].

3.3.3. *Crystalliation process*

In order to study the trend of the crystallization mechanism at each crystallization time, the enthalpy values for individual transitions for different time intervals were calculated at each crystallization temperature; the results were then plotted against the corresponding logarithm of time intervals for each member of the compound under present discussion.

Figure 10 shows such plots for BP:8ABA as a representative case of the BP:*n*ABA series at 84 and 87°C. Apart from the shift along the log *t* axis, the plots are identical in shape, suggesting the limitations of rate of crystallization [8, 9]. Moreover, the simultaneous measurement of enthalpy of the smectic G endotherm with time illustrates the effective beginning and end of the crystal formation process, which coincides with the formation of the melting transition. The plot of enthalpies of the growing melting transitions vs. log of annealing time at different crystallization temperatures is obtained by shifting the data along the log *t* axis to 87°C (figure 11). A glance at this master curve clearly shows a sudden increasing trend in the enthalpy values for lower crystallization temperatures; this provides substantial evidence towards the existence of two different crystallization mechanisms operating over the entire crystallization thermal

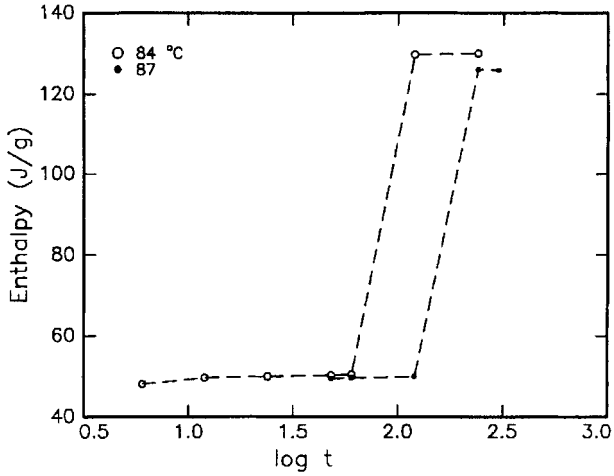

Figure 10. Heats of melting as a function of the logarithm of annealing time in the smectic G phase of BP:8ABA at 84 and 87°C.

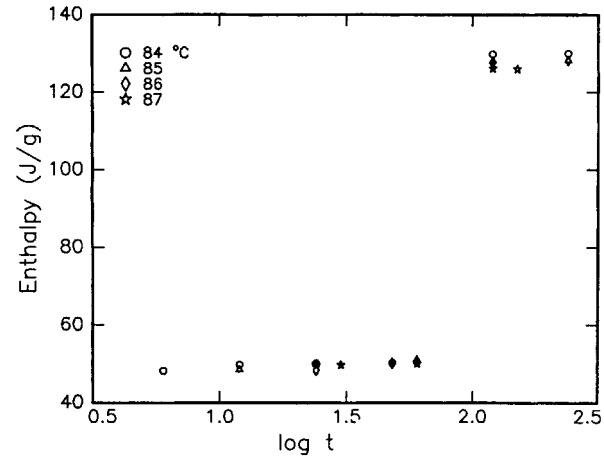

Figure 11. Master curve of enthalpies of the crystalline phase of BP:8ABA as a function of the logarithm of annealing time for different temperatures.

range. Nevertheless, the overall crystallization rate at saturation is controlled by a nucleation rate in terms of growing domains [8].

3.3.4. *Avrami parameters*

It is well known that a crystallization process involving the fraction of transformed volume x, at a time t measured since the beginning of the crystallization process, is described by the Avrami equation [16, 17]

$$x = 1 - \exp(-bt^n) \quad (1)$$

where the two constants b and n depend on the nucleation mechanism and the dimensional geometry of the growing domains, respectively.

If the kinetics of crystallization from the corresponding smectic phases are described by the above Avrami equation, the data for all the crystallization temperatures will match the single equation [18]

$$x = 1 - \exp[-(t/t^*)^n] \quad (2)$$

where $t^* = b^{-1/n}$. Further, the characteristic time t^* can be experimentally determined since at $t = t^*$, $x = 0.632$. Substituting these values of t^* and x in equation (1) constants b and n are obtained at a specified crystallization temperature.

In the present investigation the transformed volume x at a particular crystallization time is deduced from the experimental data of $\Delta H/\Delta H_o$, where ΔH is the crystal melting heat measured at time t and ΔH_0 is the maximum value obtained from the plateau of individual master curves (figure 10). The corresponding data for the compounds BP:7ABA and BP:8ABA are presented in table 2.

It is well known that the magnitude of the Avrami exponent n plays a crucial role in ascertaining the mode and class of rate transformations that occur when a stable low temperature phase grows out of a mother metastable phase in the form of small domains [15]. Diffusionless or polymorphic or cellular transformations are observed; if $n > 3$ then crystal nucleation occurs at either a constant rate or an increasing rate. For $n = 3$, nucleation occurs only at the start of the transformations. Alternatively, nucleation occurs at the start of phase transformation and continues to the grain edges or

Table 2. Crystallization parameters measured in the crystal G phase of BP:7ABA and BP:8ABA complexes.

Compound	Crystallization temperature/°C	t^*/min	x	n	b
BP:7ABA	84	2.0	0.9704	1.760	2.9×10^{-1}
	85	2.0	0.9664	1.697	3.1×10^{-1}
	86	2.0	0.9669	1.704	3.0×10^{-1}
	87	4.0	0.9533	0.766	3.5×10^{-1}
BP:8ABA	51	4.0	0.9861	0.986	2.6×10^{-1}
	52	4.0	0.6278	0.628	4.2×10^{-1}
	53	4.0	1.6275	1.627	1.0×10^{-1}
	54	32.0	0.0769	0.077	7.6×10^{-1}
	55	32.0	0.0961	0.096	7.1×10^{-1}

boundaries when $n < 3$. The lower values of n (0.5 to 2.5) favour diffusion-controlled transformations in which the nucleation starts as an initial growth of particles in the form of plates or needles of finite size possessing impinged edges.

As borne out by the data (table 2), the value of n calculated for BP:7ABA from equation (2) varies from 0.7 to 1.76, a gradual decrease in the Avrami exponent being observed with increase in crystallization temperature. This trend may be attributed qualitatively to the occurrence of a temperature dependent nucleation mechanism. The process of crystallization is assumed to follow a nucleation mode in two possible ways: (a) the growth of particles nucleated only at the start of phase transformation at the lower crystallization temperatures (CT = 84–87°C) and (b) the sudden growth of isolated plates or needles of finite size, followed by the thickening of plates after their edges have impinged when the crystallization temperature reaches 87°C. On the other hand, the low magnitudes of n in BP:8ABA (table 2) reveal the existence of a unique mode of diffusion-controlled transformation that involves the growth of isolated plates or needles possessing finite size. From the observed magnitudes of n it could be reasonable to classify the dimensionality in terms of either a two-dimensional sporadic nucleation, or growth in three dimensions. However, growth in two dimensions, favouring crystallization in smectic layers, is more probable than three-dimensional growth [8, 9].

The magnitude of constant b, which governs the nucleation mechanism, is unaltered with an order of 10^{-1} in BP:7ABA and BP:8ABA. However, in contrast to the reported analogous compounds NACP:DBA and HACP:OBA [10, 19], the constant b for the present compounds shows an altogether different trend in magnitude, a gradual increment being seen with increasing crystallization temperature (table 2). The occurrence of this reverse trend may be explained on the basis of a fast crystallization process resulting from an effective role of the less bulky bipyridyl moiety.

A quantitative approach has been made to explain the crystallization behaviour in terms of the varied magnitudes of the Avrami constant b with respect to crystallization temperature, by plotting log b at different crystallization temperatures for the compounds under discussion. The corresponding slope for each member is obtained by a linear fit which is performed to the respective values of log b and the crystallization temperature. The plots are summarized in figure 12 and reveal an interesting increasing trend in the magnitude of the slopes for BP:7ABA and BP:8ABA. In other words, it is evident that the alkoxy chain length has a pronounced impact on the nucleation mechanism. Further, the range of crystallization temperatures of the series becomes

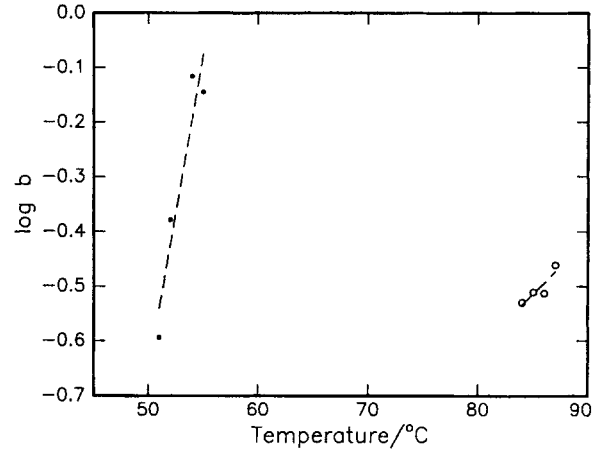

Figure 12. The logarithm of constant b as a function of crystallization temperature for BP:7ABA and BP:8ABA complexes.

broadened with the increase of alkoxy chain length. The linear nature of the curves strongly implies a unique crystallization process for the members of the series of compounds [8].

4. Conclusion

IR spectral data strongly suggest the existence of intermolecular hydrogen bonding between the ring nitrogens of 2,2′-bipyridine and the −COOH group of ABA in all the complexes of 1:2 stoichiometry. Thermal analysis reveals the induction of tilted phases, smectic F and crystal G. However, the thermal range of the nematic phase, which is a dominant phase in free *p*-*n*-alkoxybenzoic acids, is unaffected in the lower members of the series ($n = 4$ to 7). The effect of hydrogen bonding on the mesomorphism can be deduced from the phase behaviour of higher homologues where maximum thermal ranges of the induced phases are noticed.

Comparative crystallization kinetics studies performed on two homologous compounds show a crystallization mechanism operating that differs with the variation of alkoxy chain length of the benzoic acid moiety. It is further evident from the observed magnitudes of Avrami exponent n, that a temperature dependent crystallization mechanism operates in BP:7ABA. Here particles nucleate only at the start of phase transformation at the lower crystallization temperatures, with a sudden growth of isolated plates or needles of finite size. This is followed by the thickening of plates after their edges impinge when the crystallization temperature reaches 87°C. On the other hand, the low values of n in BP:8ABA reveal the existence of a unique mode of diffusion-controlled transformation that involves the growth of isolated plates or needles possessing finite size. The linear nature of plots of the Avrami constant b against crystallization

temperature also provide substantial evidence for the existence of a unique mode of crystallization operating among individual members of the series.

P.A.K. and M.S. acknowledge financial support from the Council of Scientific and Industrial Research (CSIR), New Delhi. The authors express their appreciation to Dr C. Nagaraja of S.K.D. University, Anantapur, India for his help with IR spectral recording. Financial assistance by the Department of Science & Technology and University Grants Commission (under DRS scheme), New Delhi, is also gratefully acknowledged.

References

[1] Letellier, P., Ewing, D. E., Goodby, J. W., Haley, J., Kelly, S. M., and Mackenzie, G., 1997, *Liq. Cryst*., **22,** 609.
[2] Kumar, P. A., Srinivasulu, M., and Pisipati, V. G. K. M., 1999, *Liq. Cryst*., **26,** 1339.
[3] Rudquist, P., Korblova, E., Walba, D. M., Shao, R., Clark, N. A., and Maclennan, J. E., 1999, *Liq. Cryst*., **26,** 1555.
[4] Swathi, P., Sreehari Sastry, S., Kumar, P. A., and Pisipati, V. G. K. M., *Mol. Cryst. liq. Cryst*. (to be published).
[5] Barmatov, E. G., Bobrovsky, A. Yu., Barmatova, M. V., and Shibaev, V. P., 1999, *Liq. Cryst*., **26,** 581.
[6] Sideratov, Z., Tsiourvas, D., Paleos, C. M., and Skoulios, A., 1997, *Liq. Cryst*., **22,** 51.
[7] Kato, T., and Frechet, M. J., 1989, *J. Am. chem. Soc*., **111,** 8533.
[8] Kumar, P. A., Madhu Mohan, M. L. N., and Pisipati, V. G. K. M., 2000, *Liq. Cryst*., **27,** 727.
[9] Swathi, P., Kumar, P. A., and Pisipati, V. G. K. M., 2001, *Liq. Cryst*. **28** (in press); *Phase Trans*. (in press).
[10] Srinivasulu, M., Satyanarayana, P. V. V., Kumar, P. A., and Pisipati, V. G. K. M., *Mol. Mater*. (submitted).
[11] Vogel, A. I., 1984, *Textbook of Practical Organic Chemistry*, 4th Edn (Longman).
[12] Gray, G. W., and Goodby, J. W. G., 1984, *Smectic Liquid Crystals: Textures and Structures*. (London: Leonard Hill).
[13] Silverstein, R. M., Bassler, G. C., and Morril, T. C., 1981, *Spectroscopic Identification of Organic Compounds*, 4th Edn (New York: John Wiley).
[14] Nakamoto, K., 1978, *Infrared and Raman Spectra of Inorganic and Coordination Compounds*, 4th Edn (New York: Interscience).
[15] Rao, C. N. R., and Rao, K. J., 1978, *Phase Transitions in Solids* (McGraw-Hill).
[16] Avrami, M., 1939, *J. chem. Phys*., **7,** 1103.
[17] Avrami, M., 1939, *J. chem. Phys*., **8,** 212.
[18] Ziru, H., Yue, Z., and Caille, A., 1997, *Liq. Cryst*., **23,** 317.
[19] Srinivasulu, M., Satyanarayana, P. V. V., Kumar, P. A., and Pisipati, V. G. K. M., 2001, *Z. Naturforsch*. (submitted).